ISSN 1674-1056
http://cpb.iphy.ac.cn
http://iopscience.iop.org/cpb
中国物理 B
Chinese Physics
中国物理 Chinese Physics B

Microfluidic temperature sensor based on temperature-dependent dielectric property of liquid

Qi Liu(刘琦)[1], Yu-Feng Yu(俞钰峰)[2], Wen-Sheng Zhao(赵文生)[2], Hui Li(李慧)[3]

Citation: Chin. Phys. B . 2020, 29(1): 010701 . **doi:** 10.1088/1674-1056/ab593c
Journal homepage: http://cpb.iphy.ac.cn; http://iopscience.iop.org/cpb

What follows is a list of articles you may be interested in

Low drift nuclear spin gyroscope with probe light intensity error suppression

Wenfeng Fan(范文峰)[1], Wei Quan(全伟)[1,2,3], Feng Liu(刘峰)[1], Lihong Duan(段利红)[1], Gang Liu(刘刚)[1,2,3]

Chin. Phys. B . 2019, 28(11): 110701 . **doi:** 10.1088/1674-1056/ab44a5

Observing the steady-state visual evoked potentials with a compact quad-channel spin exchange relaxation-free magnetometer

Peng-Cheng Du(杜鹏程), Jian-Jun Li(李建军), Si-Jia Yang(杨思嘉), Xu-Tong Wang(王旭桐), Yan Zhuo(卓彦), Fan Wang(王帆), Ru-Quan Wang(王如泉)

Chin. Phys. B . 2019, 28(4): 040702 . **doi:** 10.1088/1674-1056/28/4/040702

Magnetic field analysis in a diamond anvil cell for Meissner effect measurement by using the diamond NV$^-$center

Lin Zhao(赵琳), Donghui Yue(岳冬辉), Cailong Liu(刘才龙), Min Wang(王敏), Yonghao Han(韩永昊), Chunxiao Gao(高春晓)

Chin. Phys. B . 2019, 28(3): 030702 . **doi:** 10.1088/1674-1056/28/3/030702

Optical sensors based on the NiPc–CoPc composite films deposited by drop casting and under the action of centrifugal force

Noshin Fatima, Muhammad M Ahmed, Khasan S Karimov, Zubair Ahmad, Fahmi Fariq Muhammad

Chin. Phys. B . 2017, 26(6): 060704 . **doi:** 10.1088/1674-1056/26/6/060704

Ultralow detection limit of giant magnetoresistance biosensor using Fe_3O_4-graphene composite nanoparticle label

Jie Xu(徐洁), Ji-qing Jiao(焦吉庆), Qiang Li(李强), Shan-dong Li(李山东)

Chin. Phys. B . 2017, 26(1): 010701 . **doi:** 10.1088/1674-1056/26/1/010701

Microfluidic temperature sensor based on temperature-dependent dielectric property of liquid*

Qi Liu(刘琦)[1], Yu-Feng Yu(俞钰峰)[2], Wen-Sheng Zhao(赵文生)[2], and Hui Li(李慧)[3,†]

[1] School of Automation, Hangzhou Dianzi University, Hangzhou 310018, China
[2] School of Electronics and Information, Hangzhou Dianzi University, Hangzhou 310018, China
[3] School of Information and Communication Engineering, Dalian University of Technology, Dalian 116024, China

(Received 22 August 2019; revised manuscript received 4 November 2019; accepted manuscript online 20 November 2019)

We propose a low-cost compact microfluidic temperature sensor by virtue of the temperature-dependent permittivity of liquid. The sensor is composed of a coplanar waveguide (CPW) transmission line loaded with three resonators and a microfluidic plate with three channels. The resonant frequency of each resonator relies on the temperature-dependent dielectric property of liquid in corresponding channel, which therefore can be used to extract the temperature. The proposed sensor features a compact size and low cost since it requires only micro fluid volume instead of additional electronic components to produce significant frequency shift with changing temperature. Moreover, it exhibits decent accuracy and stability in a temperature sensing range from 30 °C to 95 °C. A theoretical analysis of the sensor is provided, followed by the detailed characterization method, and a prototype is designed, manufactured, and measured to verify the theoretical analysis.

Keywords: microfluidics, sensors, permittivity, dielectric liquid

PACS: 07.07.Df, 07.50.–e **DOI:** 10.1088/1674-1056/ab593c

1. Introduction

Microfluidics is the science and technology of systems that process or manipulate small amounts of fluids, by using channels with dimensions of tens to hundreds of micrometers.[1] With the introduction of microfluidics, fluid analysis can be performed on samples of microliter-order due to the monolithic integration of sensing and interface electronics, fluidic manipulation structures, and micrometer-sized fluid channels on a single packaged chip.[2–5]

Over the past decades, microfluidics has been adopted in a number of different kinds of sensors by turning the fluid information into electromagnetic signals.[6] For example, in one of the first micromechanical flow sensors for liquids,[7] the flow in the microfluidic channel was measured as a phase shift. In the sweat electrolyte sensor,[8] the Na^+ concentration of the sweat in the microfluidic channel was turned into the potential across the electrode–ionophore barrier. A reasonace-based microfluidic device was utilized for characterizing the complex permittivity based on the measurement of the resonant frequency and associated attenuation.[9] The nanoliter liquid interdigitated capacitor was evaluated to accurately characterize the referenced binary liquid mixtures by capacitance and conductance contrast spectrum.[10] The frequency shift of a voltage-controlled oscillator was used to measure the complex permittivity of lossy organic liquids.[11] These microfluidic sensors have many advantages, such as low profile and compact size to miniaturize the device, easy integration into RF systems, non-invasive installation, and real-time reaction to the changes of the liquids.

Apart from the above sensors which mainly detect the properties or conditions of the liquid in microfluidic channels, the microfluidic sensors can also take advantage of some environment or interaction dependent properties of the liquid to realize environment or interaction detections. Taking the extensively used temperature sensor for example, instead of direct integration of electronic temperature sensing devices such as thermocouples/thermopiles, thermistors or resistance temperature detectors,[12–14] the temperature sensor[15] utilized the thermal volume expansion of liquid metal in microfluidic channels into a progressively short circuit, a linear array of dipoles, so that their aggregate radar cross section would effectively increase or decrease with temperature increasing. The capacitive temperature sensor[16] was based on an interdigital capacitor with a microfluidic channel between the two electrodes, and the temperature-dependent dielectric constant of the PDMS fluid in the channel would affect the capacitance. In the millimeter-wave microfluidic temperature sensor,[17] the water level in the channel would rise across the capacitor plates with the expansion of temperature-dependent volume, and this rising level of high permittivity liquid within the capacitor modified the capacitance and the scattering parameter.

In this paper, a novel microfluidic temperature sensor is

*Project supported by the Natural Science Foundation of Zhejiang Province, China (Grant No. LQ19F010007), the National Natural Science Foundation of China (Grants Nos. 61901146 and 61874038), and the Smart City Collaborative Innovation Center of Zhejiang Province, China.

†Corresponding author. E-mail: Hui.li@dlut.edu.cn

© 2020 Chinese Physical Society and IOP Publishing Ltd

proposed. It is based on multi-resonators loaded in a coplanar waveguide (CPW) transmission line and takes advantage of the temperature-dependent permittivity of liquid to produce significant frequency shift with temperature changing. Compared with the temperature sensors in Refs. [15–17] it features low cost, batch production, expandability, and easy integration due to its CPW structure and low-priced fabrication process, and it exhibits decent accuracy and stability in a temperature sensing range from 30 °C to 95 °C. More importantly, the proposed sensor is workable in different ambient conditions according to our characterization method in this paper, whereas the sensors in Refs. [15–17] still need calibration to deal with possible measurement deviation caused by ambient interference, which has rarely been taken into account in previous works.

2. Configuration and mechanism

The proposed prototype consists of a CPW structure and a microfluidic plate as shown in Fig. 1(a). The CPW transmission line with three meandered lines loaded in the slots of signal line (1st layer) is printed on the substrate of polyethylene terephthalate (PET) (2nd layer), and the polypropylene (PP) film (3rd layer) is used to seal the polymethyl methacrylate (PMMA) plate engraved with three microfluidic channels (4th layer). The inlets and outlets of the channels are drilled from the bottom surface of the plate. The microfluidic channels are complementary to the meander-lines in structure. In other words, the microfluidic channels are located just beneath the resonating elements and fill the gaps of the vertical projections of the meander-lines in the top view of the prototype as shown in Fig. 1(b). It is because the current is distributed mainly in the meander-lines of the resonating element

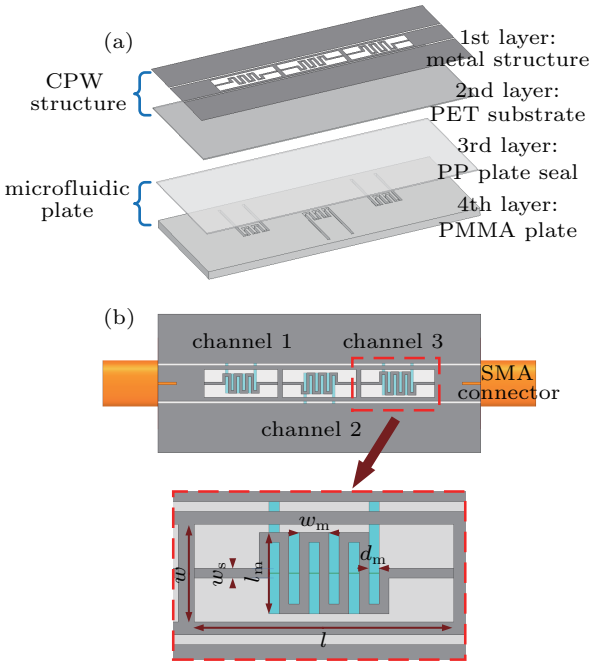


Fig. 1. (a) Hierarchical three-dimensional view and (b) top view and parameter setting of the proposed sensor.

as shown in Fig. 2. With this channel arrangement, the liquid in the channels could affect the main current paths of the resonating elements.

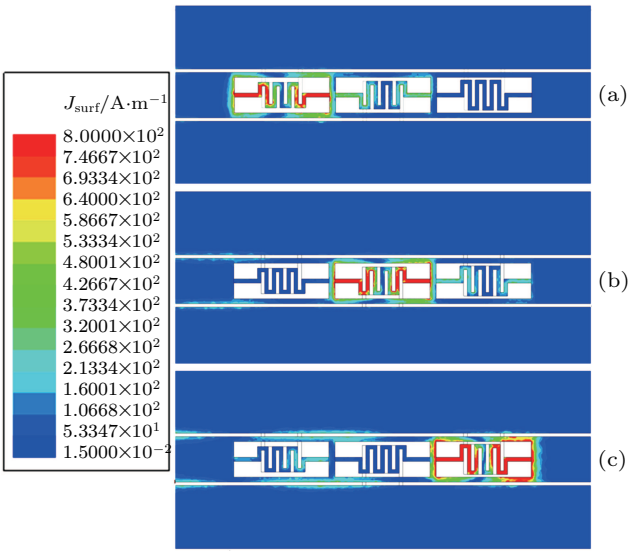


Fig. 2. Current distribution of the CPW transmission line with three meandered lines at resonance frequencies of (a) element 1, (b) element 2, and (c) element 3.

The dielectric properties and thickness of different material layers are given in Table 1.

Table 1. Dielectric properties and thicknesses of material layers used in proposed sensor.

Material	PET	PP	PMMA
Relative permittivity	3.2	2.6	3.4
Loss tangent	0.003	0.0002	0.04
Thickness/mm	0.05	0.05	1

According to processing requirements and parametric study results, the CPW transmission line has a signal line width of 3.8 mm and gap between signal line and ground of 0.3 mm, and the microfluidic channels each feature 300-μm width and 400-μm height. As shown in Fig. 1(b), the parameters of for each of the resonating elements are determined as follows: $w = 3$ mm, $l = 8$ mm, $w_s = 0.3$ mm, $w_m = 0.9$ mm, $d_m = 0.3$ mm. It is noticeable that the three meandered lines have different length (l_m) values of 2.1 mm, 2.3 mm, and 2.5 mm while other parameters remain the same.

In order to explain the mechanism of the sensor, the capacitance C_m and the inductance L_m of the meander-line are studied based on the parallel plate transmission line. The values of C_m and L_m can be estimated by the following equations:[18]

$$C_m = \varepsilon_r \varepsilon_0 \frac{t_{met} l_m}{N d_m}, \tag{1}$$

$$L_m = \mu_r \mu_0 \frac{N d_m l_m}{t_{met}}, \tag{2}$$

where t_{met} is the thickness of metal, N is the number of line lengths, ε_0 and μ_0 are respectively the permittivity and permeability of free space, ε_r and μ_r are respectively the effective

relative permittivity and permeability of the multi-layer substrate including the liquid in the microfluidic channels.

From Eqs. (1) and (2), we can see that the three resonant elements with different values of meandered length l_m will have different resonant frequencies, and for a single resonant element with fixed dimension parameters, the variable permittivity of liquid caused by temperature variation will also lead to different resonant frequencies. Therefore, the temperature can be theoretically identified by the frequency spectrum of the sensor.

3. Prototype fabrication and analysis

The fabrication of microfluidic devices usually is divided into two parts: the fabrication of microfluidic channels and fabrication of interface metal structures. The key fabrication process of microfluidic channels is the photolithography, in which the microstructures are patterned by exposing and developing. Interface metal structure is usually thin-film deposited with physical vapor deposition (PVD) technique (such as thermal evaporation and sputtering) or photolithographically patterned.[19,20] However, these processes mostly require a controlled laboratory environment and expensive equipment, which leads to high cost and low production of the microfluidic devices.

In order to reduce the cost and achieve mass production of the proposed sensor, the CPW structure (1st and 2nd layers in Fig. 1) and the microfluidic plate (3rd and 4th layers) of the prototype are fabricated separately with different processes. The CPW structure of the prototype is fabricated in a roll-to-roll (R2R) screen printing process.[21] The microfluidic channels are carved on the PMMA plate with a numerically controlled (NC) machine, then the PP film is hot-pressed to seal the PMMA plate. After completion of separate processing, the CPW structure is attached to the microfluidic plate with 0.02 mm-thick PET adhesive. Finally, the liquid is injected into the microfluidic channels by pipette, the inlets and outlets of channels at the bottom of the plate as shown in Fig. 3(a) are sealed by resin adhesive. The finished prototype is presented in Fig. 3(b).

The processes adopted in the fabrication (R2R process and NC maching) prove to be cheap and mass productive, which is required by numerous industrial applications, therefore the low cost and high volume of our proposed sensor can be achieved.

To characterize the temperature from the frequency spectrum of the sensor, an accurate relationship between the temperature and resonant frequency should be established theoretically, and theoretical simulated values and experimental results are predicted to be in good agreement. So the simulated and measured transmission coefficients of the proposed sensor with no liquid in the channels are compared with each other to verify the coincidence between simulation result and measurement result.

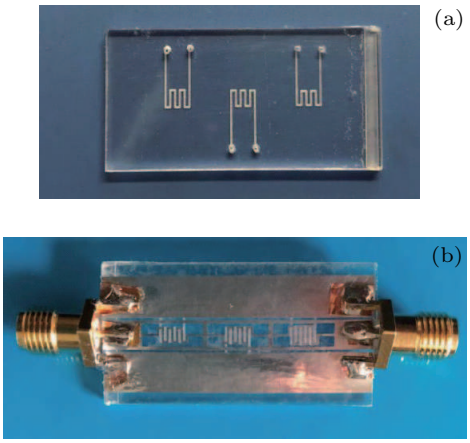


Fig. 3. Prototype of (a) microfluidic plate (bottom view) and (b) proposed sensor (top view).

However, as shown in Fig. 4, there is a frequency deviation between the simulations and measurements of the transmission coefficient. It is mainly caused by the difference in material permittivity between batches and ambient interference, the errors introduced by the fabrication process, and machining precision, which leads the frequency deviation to be difficult to avoid. Therefore, additional error will be inevitably introduced into the relationship between the temperature and resonant frequency.

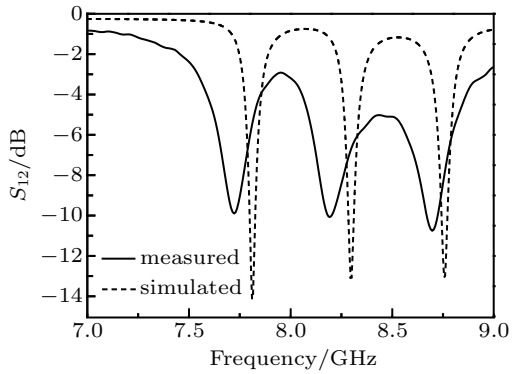


Fig. 4. Simulated and measured results of transmission coefficient of proposed sensor without liquid in channels.

4. Simulation and characterization

According to the analysis on Fig. 4, the resonant frequency is not suitable for characterizing the temperature. The frequency shift with temperature changing is considered as a more suitable indicator to characterize temperature since based on experience the deviation could be eliminated by subtraction. An accurate corresponding relationship between the frequency shift and temperature will be established to prove this characterization method in this section.

The distilled water is chosen as the liquid in the microfluidic channels in this design since there is sufficient information about the permittivity of water in the existing literature. The

relative permittivity of water is given according to the Debye relaxation model[22]

$$\varepsilon' = \varepsilon_\infty + \frac{\varepsilon_s - \varepsilon_\infty}{1+(\omega\tau)^2}, \tag{3}$$

where $\omega = 2\pi f$ is the radian frequency with f being in Hz, ε_∞ is the dielectric constant at infinitely high frequency, ε_s is the static dielectric constant, and τ is the relaxation time in second.

For distilled water, it is assumed that $\varepsilon_\infty = 4.9$, the regression equations of the static dielectric constant and relaxation time of distilled water are given by 3rd order regression fit[23]

$$\begin{aligned}\varepsilon_s &= 88.045 - 0.4147T + 6.295\times10^{-4}T^2 \\ &\quad + 1.075\times10^{-5}T^3, \end{aligned} \tag{4}$$

$$\begin{aligned}\tau &= 1.768\times10^{-11} - 6.086\times10^{-13}T + 1.104\times10^{-14}T^2 \\ &\quad - 8.111\times10^{-17}T^3. \end{aligned} \tag{5}$$

According to Eqs. (3)–(5), besides the significant influence of temperature, the permittivity of distilled water also receives a minor influence of frequency as shown in Fig. 5. Since the resonant frequency of the sensor is still unknown, the average permittivity between 30 °C–95 °C in Fig. 5 is adopted in the simulation with Ansoft HFSS to estimate the medians of the resonant frequencies of different resonating elements with their corresponding channels filled by distilled water.

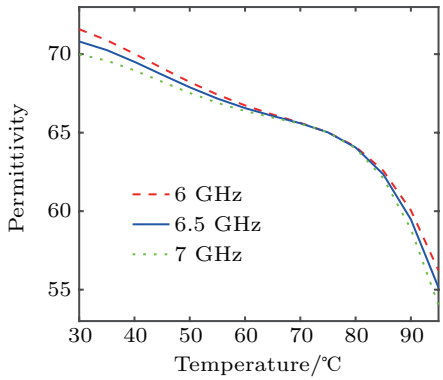


Fig. 5. Temperature-dependent permittivity of distilled water at different frequencies.

Then the permittivity values of distilled water at different temperatures can be calculated from Eqs. (3)–(5) according to the simulated medians of resonant frequencies. After that, the permittivity values are introduced into the simulation with Ansoft HFSS. The temperature range in simulation is set to be 30 °C–95 °C since the heating plate used in the following experiment only supports the temperatures above room temperature.

The simulated frequency shifts of different resonating elements with corresponding channels filled by distilled water are shown in Fig. 6. The results exhibit a significant consistency except some minor deviations mainly due to calculation and simulation errors. It indicates that there is a homologous mathematical relationship between the frequency shift and temperature, which is unrelated to the initial resonant frequency. Thus, the temperature can be characterized by corresponding frequency shift.

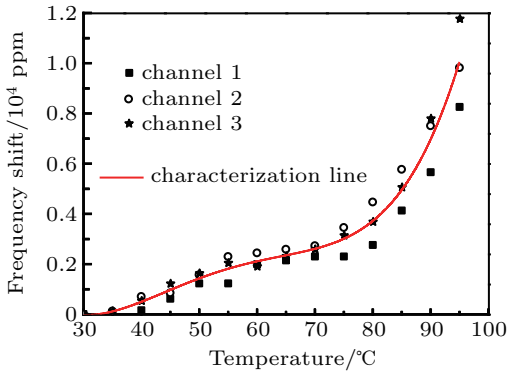


Fig. 6. Simulation results of frequency shift *versus* frequency and regression fitted characterization line of proposed sensor.

A fitted curve of the averaged simulation results is given by Eq. (6) and plotted in Fig. 6 as well, and shows the 4th order temperature-dependency of the frequency shift. This curve is the characterization line of the proposed sensor which could be used to extract temperature from the measured frequency shift:

$$\Delta f(\text{ppm}) = a + bT + cT^2 + dT^3 + eT^4. \tag{6}$$

Table 2. Parameters of Eq. (6) calculated from average of simulation results.

a	b	c	d	e
18395.08014	−1645.10081	51.29143	0.6548	0.00303

5. Experiment and discussion

To test the accuracy of the characterization line, the proposed sensor is applied to a temperature sweep from 30 °C to 90 °C in steps of 10 °C by using a Thermo Scientific Cimarec heating plate, and the transmission coefficient is measured by Agilent E8358A. The measured resonant frequencies of three resonating elements with channels 1–3 are converted into frequency shifts, and the temperatures are retrieved directly from the characterization line according to their corresponding frequency shifts.

The temperatures measured in the experiments and their test errors are listed in Table 3. Although the temperature can be obtained by a single resonating element with corresponding microfluidic channel alone, averaged temperature obtained by different resonating elements tends to improve the accuracy. The maximum test error reduces from 11.2% (a single resonating element with channel 3) to 5.31% (average of three sets of measured temperatures).

The accuracy of the characterization line derived from the regression fit curve of the simulation results is not so satisfactory compared with those from some traditional temperature

sensors. It is mainly because the temperature-dependent permittivities of the substrate materials (PP, PET, and PMMA) used in this sensor can also result in slight frequency shifts, although their values are quite small compared to the permittivity of water results in. However, it is difficult to quantify the influence of substrate material on the frequency shift in the equation since there is limited material property data about PP, PET, and PMMA, and the structure of the proposed sensor is complex, so that only the temperature-dependent permittivity of liquid in microfluidic channels is taken into consideration in the simulation and the characterization line.

Table 3. Measured temperatures and test errors of different resonating elements with channels 1, 2, and 3.

Temperature/°C	30	40	50	60	70	80	90
Channel 1	28.87	40.45	47.44	56.92	62.24	78.88	94.53
|Error1|/%	3.77	1.13	5.12	5.13	11.09	1.40	5.03
Channel 2	28.87	42.30	51.58	55.90	68.13	82.59	92.05
|Error2|/%	3.77	5.75	3.16	6.83	2.67	3.24	2.28
Channel 3	28.87	35.52	52.22	57.62	70.42	76.53	91.21
|Error3|/%	3.77	11.20	4.44	3.97	0.60	4.34	1.34
Average	28.87	39.42	50.41	56.81	66.93	79.33	92.60
|Error|/%	3.77	1.44	0.83	5.31	4.39	0.83	2.89

Fortunately, the Debye relaxation model is also suitable for the permittivities of PP, PET, and PMMA,[24–26] the analytical and measurement method of the sensor are still tenable with consideration of the substrate material, and the accuracy of the characterization line can be improved by modifications of the parameters in Eq. (6) according to the fit curve of multiple actual experiment results.

Besides the distilled water, many more kinds of liquids (or mixtures) with temperature-dependent permittivity can also be adopted in the proposed sensor, such as glycerol or water-methanol mixture. Since the permittivity of different liquid shows different temperature-dependency, changing the liquid types in one or more microfluidic channels could be helpful in further increasing the accuracy of the proposed sensor.

6. Conclusions

In this paper we proposed a low-cost compact microfluidic temperature sensor which supports reliable temperature sensing in a range between 30 °C–95 °C. The sensor takes advantage of the temperature-dependent permittivity of liquid in microfluidic channels instead of thermosensitive components. It requires only micro fluid volume to produce significant frequency shift with temperature changing and exhibits decent accuracy and stability in temperature sensing. The CPW structure and compact size allow the sensor to be easily integrated into a system or combined with RFID/Bluetooth/Zigbee module to develop into an on-chip sensor or a wireless sensor. Moreover, the advantages of low-cost and mature processes make it suitable for mass productions and wide applications.

References

[1] Whitesides G M 2006 *Nature* **442** 368

[2] Cook B S, Cooper J R and Tentzeris M M 2013 *IEEE Trans. Microwave Theory Tech.* **61** 4714

[3] Li L and Zhang C B 2018 *Acta Phys. Sin.* **67** 176801 (in Chinese)

[4] Min L L, Chen S Y, Sheng Z Z, Wang H L, Wu F, Wang M and Hou X 2016 *Acta Phys. Sin.* **65** 178301 (in Chinese)

[5] Gao A R, Liu X, Gao X L, Li T, Gao H M, Zhou P and Wang Y L 2011 *Chin. Phys. Lett.* **28** 084706

[6] Abduljabar A A, Rowe D J, Porch A and Barrow D A 2014 *IEEE Trans. Microwave Theor. Tech.* **62** 679

[7] Branebjerg J, Jensen O S, Laursen N G and Leistiko O 1991 *IEEE International Conference on Solid-state Sensors & Actuators,* June 24–27 1991, San Francisco, CA, USA, p. 41

[8] Rose D P, Ratterman M E, Griffin D K, Hou L L, Kelley-Loughnane N, Naik R R, Hagen J A, Papautsky I and Heikenfeld J C 2015 *IEEE Trans. Biomed. Eng.* **62** 1457

[9] Chretiennot T, Dubuc D and Grenier K 2013 *IEEE Trans. Microwave Theor. Tech.* **61** 972

[10] Chen T, Dubuc D, Poupot M, Fournié J and Grenier K 2012 *IEEE Trans. Microwave Theor. Tech.* **60** 4171

[11] Sekar V, Torke W J, Palermo S and Entesari K 2012 *IEEE Trans. Microwave Theor. Tech.* **60** 1444

[12] Zhang Y and Tadigadapa S 2004 *Biosens. Bioelectron* **19** 1733

[13] Ernst H, Jachimowicz A and Dynamic G 2001 *IEEE Sens. J.* **1** 361

[14] Fürjes P, Légrádi G, Dücso C, Aszódi A and Bársony I 2004 *Sensors and Actuators A (Physical)* **115** 417

[15] Traille A, Bouaziz S, Pinon S, Pons P and Tentzeris M 2011 *IEEE 41st European Microwave Conference (EuMC)*, October 10–13, 2011, Manchester, UK, p. 45

[16] Rifai A, Debourg E, Bouaziz S, Traille A, Pons P, Aubert H and Tentzeris M 2013 *The 17th International Conference on Solid-State Sensors, Actuators and Microsystems*, June 16–20, 2013, Barcelona, Spain, p. 1024

[17] Bouaziz S, Chebila F, Traille A, Pons P, Aubert H and Tentzeris M 2012 *IEEE Sens.*, October 28–31, 2012, Taipei, Taiwan, China

[18] Murji R and Deen M J 2002 *IEEE Trans. Electron. Dev.* **49** 187

[19] Leester-Schädel M, Lorenz T, Jürgens F and Richter C 2016 *Microsystems for Pharmatechnology* (Cham: Springer) pp. 23–57

[20] Hu J, Deng X, Sang S B, Li P W, Li G and Zhang W D 2014 *Acta Phys. Sin.* **63** 207102 (in Chinese)

[21] Salam B, Shan X C and Jun W 2016 *IEEE 18th Electronics Packaging Technology Conference (EPTC)*, November 30–December 3, 2016, Singapore, Singapore, p. 250

[22] Agmon N 1996 *J. Phys. Chem.* **100** 1072

[23] Klein L and Swift C 1977 *IEEE Trans. Anten. Propag.* **25** 104

[24] Drozdov A D and Dusunceli N 2012 *Iranian Polym. J.* **21** 701

[25] Pop T, Iordache D and Jonas A 1997 *Microelectron. Eng.* **33** 377

[26] Lin K C and Aklonis J J 1981 *Polym. Eng. Sci.* **21** 703